

# Theory of the effect of light scattering from dispersed pigment particles on hard copy monochrome color

Robert J. Meyer  
 Xerox Corporation  
 Webster, NY USA

## Abstract

In this talk we first assess the use of the Williams-Clapper [1] model for first-principles calculation of CIELAB color coordinates of hard copy xerographic monochrome images. This model produces color coordinates  $a^*$  and  $b^*$  which are in good agreement with the observed colors for xerographic monochrome images. Typical chroma errors produced by this model are on the order of  $\Delta C^* = 5$ , with an equal spread both above and below the observed values. However, the Williams-Clapper model does not make accurate predictions for the image lightness  $L^*$ . Typical lightness errors are on the order of  $\Delta L^* = 15$ , and the predicted lightness is always too low; too little light is predicted to be reflected. We attribute this failure to the lack of backscattered light from embedded pigment particles.

We modify the Williams-Clapper model by including the scattering of light from dispersed pigment particles in the fused toner layer. Renormalization group techniques are used to include all orders of light scattering between the front surface, the pigment particles in the image, and the rough paper surface. The model presented here reduces to the Williams-Clapper model in the limit that scattering from the pigment particles vanishes.

## Introduction

Williams and Clapper [1] propose a model of the reflectivity of a color print, which is quite successful in predicting the optical density of photographic color prints. The model, illustrated in Fig. 1, includes multiple reflections of light to all orders between the front image surface (assumed to be smooth), and the rough paper surface. In this model all diffuse scattering of light, which is the light measured for colorimetric purposes, results from scattering from the rough paper surface. Since the front surface is specular, only light scattered from paper at or near normal incidence is measured in color measurements.

Williams and Clapper are primarily concerned with explaining the whiteness observed in highlight areas of photographic prints. In such areas there are no absorbing dyes or silver grains, and thus, no backscatterers between the image surface, and the paper.

A simple optical model for the reflectivity results in a single integral equation for the image reflectivity,  $R$ .

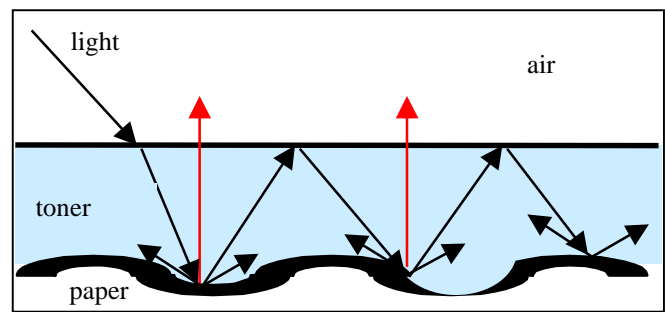


Figure 1. Schematic illustration of light scattering in the Williams and Clapper [1] model, showing multiple reflections of light between image surface and paper. Typically only light leaving within a narrow angular range around the normal to the surface (the red rays) contribute to color measurements.

This equation is easily solved to yield:

$$R = \frac{T_{air-image}(\theta_1, \theta_2) t^{1+\sec(\theta_2)} R_{paper}(\theta_2, 0, \lambda) T_{image-air}(0, 0)}{1 - \int d\Omega_3 R_{1Down}(\theta_2, \theta_3) t^{2\sec(\theta_2)} R_{paper}(\theta_2, \theta_3, \lambda)} \quad (1)$$

where  $\theta_1$  is the angle of the incident light on the color image with respect to the normal to the surface,  $\theta_2$  is the angle of the light after specular transmission through the surface, and  $\Omega$  is a solid angle.  $R_{1Down}$  is the specular reflection coefficient of the image surface for light within the image reflecting off the interface with air,  $R_{paper}$  the diffuse reflection coefficient of the paper, which is assumed to be a Lambertian reflector.  $T_{air-image}$  is the transmission coefficient for light going from the air into the toned image, and  $T_{image-air}$  is the transmission coefficient for light going from the toned image into the air. In Eq. (1)  $t$  is the transmission coefficient of the image layer for light traveling *normal* to the surface. The exponent  $\sec(\theta_2)$  incorporates the effect of the increased light absorption for light traveling at an angle  $\theta_2$  with respect to the normal to the surface.

The Williams-Clapper model assumes a smooth front surface; all diffuse scattering is a result of scattering from

the rough paper surface. The Williams-Clapper model has been modified to include the effects of a rough front image surface by Takahashi [2].

Within the Williams-Clapper model paper is assumed to be a Lambertian reflector. This simplifies Eq. (1) to:

$$R = \frac{T_{air-image}(\theta_1, \theta_2) t^{1+\sec(\theta_2)} R_{paper}(\lambda) T_{image-air}(0,0)}{1 - R_{paper}(\lambda) \int d\Omega_3 R_{Down}(\theta_2, \theta_3) \cos(\theta_3) t^{2\sec(\theta_3)}} \quad (2)$$

The only inputs to the color model in this analysis are:

- (i) the measured pigment complex dielectric constants;
- (ii) the measured complex dielectric constant of the binder;
- (iii) the volume fractions of the pigment present;
- (iv) the wavelength dependent reflectivity of the paper; and
- (v) the mass per unit area of the toner on paper.

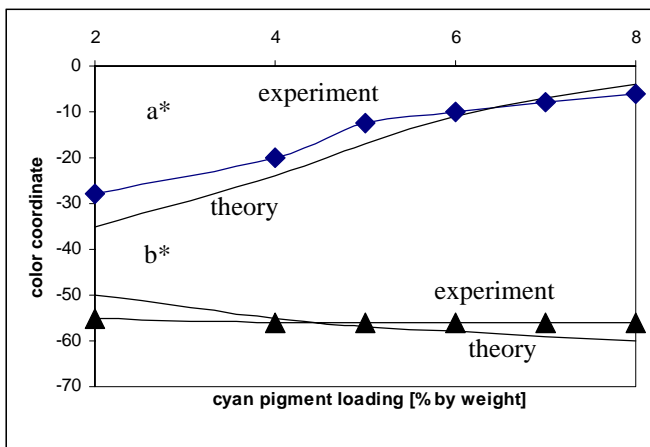


Figure 2. Comparison between the Williams and Clapper theory and experiment for a\* and b\*. The rms error in each case is on the order of 5 color units.

In Figs. 2 and 3 we illustrate the effects of varying the cyan pigment loading from 2% by weight to 8% by weight. As we see from the figure, the trends predicted by the model, increasing a\* and decreasing b\* with increasing pigment loading, are in qualitative agreement with the data. The rms errors in chroma, ΔC\*, are approximately 5 color units. Also, the predicted and observed lightness coordinates L\* also have similar trends with increased pigment loading: the lightness L\* drops as more absorbing pigment is added. However, the lightness predicted by the model is too low by up to 15 color units.

The dominant error in the Williams-Clapper analysis is that the predicted lightness is monotonically low for all pigment loadings. There is no monotonic error in a\* and b\* as predicted by the model: sometimes a\* (or b\*) is high, sometimes low. Thus, the model is at least approximately correct. In the next section we discuss an extension to the

Williams and Clapper model that will increase the predicted amount of light reflected from a toned surface.

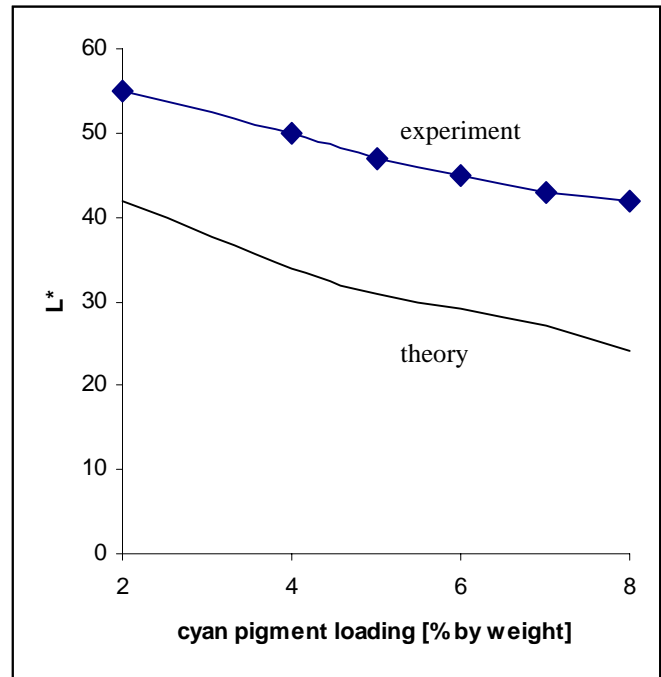


Figure 3. Comparison between the Williams and Clapper theory and experiment for L\*.

### Revised model for hard copy monochrome color

The observations above suggest that too little light is being reflected into the diffuse normal direction in the Williams-Clapper model. Three possible mechanisms, which would produce increased backscattering of light, come to mind:

- (i) Williams and Clapper assume the front surface of the image is smooth, i.e., specular. As a result there is no contribution to the diffuse intensity (i.e., color) from the front surface.
- (ii) Light backscattered from pigment particles is not considered. Pigment particles only contribute to absorption of light in the toner layer in the Williams-Clapper model.
- (iii) Light backscattered from internal air pockets and other structural imperfections are not considered.

Effect (i) above has been considered by Takahashi [2]. In the present case we find that front surface reflection effects are too small to explain the difference between the predicted and observed L\* values.

In some sense, items (ii) and (iii) above are identical, light scattering from inhomogeneities in the image layer. In this paper we derive equations specifically for the effects of light scattering from pigment particles. However, these same equations can be used to describe the effects of inclusions (spherical inclusions in the analysis presented

here) such as dust particles or (spherical) air bubbles, such as might occur in poorly fused xerographic images.

The light scattering processes we add to the Williams-Clapper model are indicated in the top panel of Fig. 4. These are light scattering from a disordered layer of pigment particles, located between  $x_1$  and  $x_1 + \delta x_1$  from the front surface of the image. The reflectivity of the image is now made up of component light scattering processes, as indicated in the lower panel of Fig. 4. The only contributions to the measured diffuse color reflectance signal in this diagram are those reflected in a small angular range around normal to the surface from either the paper or from the fictitious "pigment layer". In the figure, we show only a single pigment layer. In actuality, we must integrate the position of the pigment layer from zero to the total thickness of the toner layer to include all effects of pigment scattering. In addition, we must include light scattering from one pigment layer, reflecting from either the front surface or paper, and scattering from another pigment layer. This is done by the way the spatial integrals are structured in the following analysis.

In the light scattering component processes indicated in Figs. 4 and 5 light flux is conserved at each interface. However,

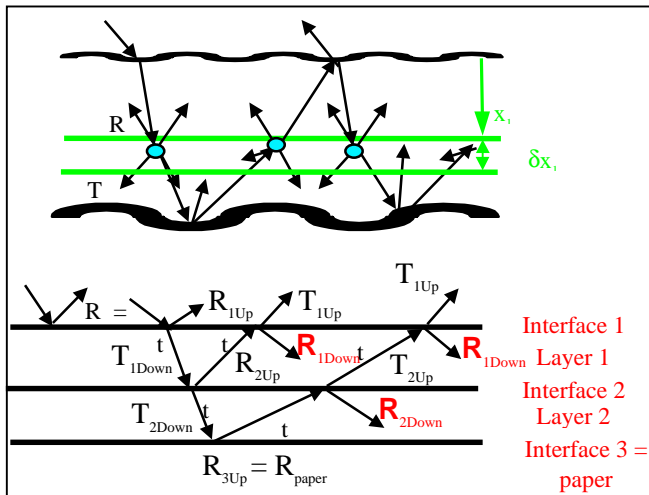


Figure 4. The top panel illustrates the scattering of light from pigment particles embedded in the image, in addition to light scattering from the front image surface and the paper. The bottom panel illustrates the component processes that contribute to the image reflectivity  $R$ . The bold red Helvetica font  $R$ 's indicate renormalized reflectivities, i.e., the reflectivities that include infinite multiple relectivity components.

flux is not conserved in traversing the toner layer due to the frequency-dependent light absorption contained in the  $t$  transmission coefficient.

Note that for this monochrome (i.e., 1-color) problem the structure of the image gives three interfaces, two layers, and one distinct value of the normal incidence layer transmission coefficient  $t$ . In the general four-color problem

a similar analysis involves multiple scattering from nine interfaces, eight layers, and four distinct values of  $t_i$ .

Just as there was multiple reflection of light between the image front surface and the paper in the Williams-Clapper model, in the present model we must also include this multiple reflection of light. Only now we must include multiple reflections between three interfaces: paper, front surface, and pigment layers. We do this by using a technique used in solid state and particle physics, that of *renormalized* scattering (in this case reflection) vertices (Brown[3]). There are integral equations that these renormalized reflection coefficients must obey, corresponding to their graphical structure as illustrated in Fig. 5. If these graphs (and equations) are recursively substituted into themselves wherever they appear, a multiple scattering form becomes

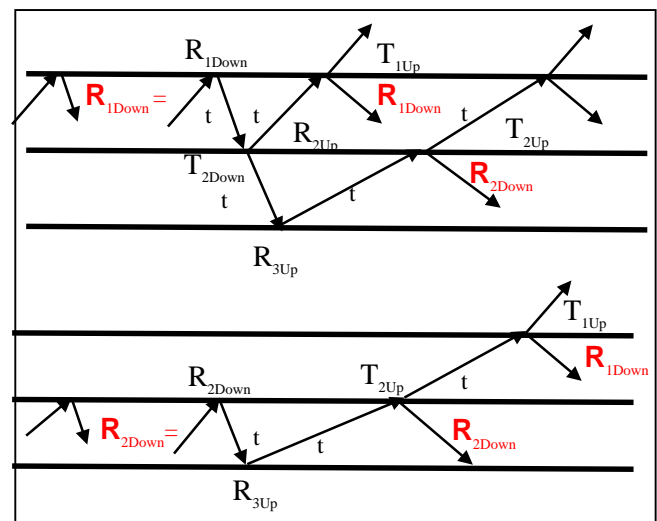


Figure 5. Schematic illustration of the renormalized reflection coefficients used to include multiple reflection events between the front image surface and the pigment layer (upper panel) and the paper and the pigment layer (lower panel). Note that the two renormalized reflectivities are coupled.

apparent that accurately describes the corresponding physical process.

In order to describe the multiple reflections within and between two layers it is necessary to renormalize two reflection coefficients. In the analysis given here we have chosen to renormalize the  $R_{1Down}$  and  $R_{2Down}$  reflection coefficients. This was not the only possible choice. We could have equally well have chosen to renormalize  $R_{3Up}$  or  $R_{2Up}$ . The present choices were made because the structure of the resulting equations was simplest for this choice. The same physical results, i.e., reflectivity, could be obtained by other choices: this analysis is not unique.

The goal of this report is to write down, in closed form, a set of expressions that represents the multiple scattering processes indicated in Fig.4., i.e., the total intensity from all orders of multiple scattering within the xerographic monochrome image. That result is given by:

$$\begin{aligned}
 R(\theta_p, 0) &= R_{1Up}(\theta_p, 0) + T_{1Down}(\theta_p, \theta_2) \int dx_1 t(x_p, \theta_2) \\
 &[\int d\Omega_3 T_{2Down}(\theta_2, \theta_3) t(x_p, \theta_3) \int d\Omega_4 R_{3Up}(\theta_3, \theta_4) \int dx_2 t(x_2, \theta_4) \\
 &\{ \int d\Omega_5 T_{2Up}(\theta_p, 0) t(x_2, 0) (T_{1Up}(0, 0) + \int d\Omega_6 \mathbf{R}_{1Down}(\theta_3, \theta_6)) + \mathbf{R}_{2Down}(\theta_p, \theta_3) \} \\
 &+ R_{2Up}(\theta_2, 0) t(x_p, 0) (T_{1Up}(0, 0) + \int d\Omega_7 \int d\Omega_8 \mathbf{R}_{1Down}(\theta_7, \theta_8))], \quad (3)
 \end{aligned}$$

where  $\mathbf{R}_{1Down}$  and  $\mathbf{R}_{2Down}$  are renormalized reflectivities. Note that the renormalized reflectivities are indicated by both a different typeface (**Bold Helvetica**) and red color. The meaning of these renormalized reflectivities is clarified below. [Note that in Eq. (3), and in the remainder of this paper,  $t$  is the transmission coefficient for light propagating at an angle to the image surface. The  $\sec(\theta)$  exponent of Eqs.(1) and (2) has been absorbed into the  $t$  for simplicity of notation.]

Light does not can cross back and forth between the layers. This results in coupling of the equations for the renormalized reflectivities. The renormalized reflection amplitude  $\mathbf{R}_{1Down}$  must satisfy:

$$\begin{aligned}
 \mathbf{R}_{1Down}(\theta_p, \theta_2) &= R_{1Down}(\theta_p, \theta_2) t(\theta_2) \int d\Omega_3 \int d\Omega_4 [T_{2Down}(\theta_2, \theta_3) t(\theta_3) \\
 &R_{3Up}(\theta_3, \theta_4) \\
 &\int dx_2 t(\theta_4) \int d\Omega_5 \int d\Omega_6 \{ T_{2Up}(\theta_2, \theta_3) t(\theta_3) (T_{1Up}(\theta_3, 0) + \mathbf{R}_{1Down}(\theta_3, \theta_6)) + \\
 &\mathbf{R}_{2Down}(\theta_p, \theta_3) \} + R_{2Up}(\theta_2, \theta_3) t(\theta_3) (T_{1Up}(\theta_3, 0) + \mathbf{R}_{1Down}(\theta_3, \theta_4))]. \quad (4)
 \end{aligned}$$

Similarly,  $\mathbf{R}_{2Down}$  must satisfy:

$$\begin{aligned}
 \mathbf{R}_{2Down}(\theta_p, \theta_2) &= R_{2Down}(\theta_p, \theta_2) t(\theta_2) \int d\Omega_3 \int d\Omega_4 R_{3Up}(\theta_2, \theta_3) \int dx_3 t(\theta_3) \\
 &[T_{2Up}(\theta_p, \theta_4) t(\theta_4) (T_{1Up}(\theta_p, 0) + \int d\Omega_5 \mathbf{R}_{1Down}(\theta_p, \theta_5)) + \mathbf{R}_{2Down}(\theta_p, \theta_4)]. \quad (5)
 \end{aligned}$$

Note that the  $\mathbf{R}_{1Down}$  reflectivity equation is coupled to the  $\mathbf{R}_{2Down}$  reflectivity. Thus, we have two coupled integral equations in two unknown functions,  $\mathbf{R}_{1Down}$  and  $\mathbf{R}_{2Down}$ . When these two coupled equations are solved, the solutions are substituted into Eq. (3) to give the image reflectivity.

The coupled integral equations for the renormalized reflectivities can be solved analytically by converting the integral equations to matrix equations. This is accomplished by converting the integrals in Equations (4) and (5) to sums over angular ranges, and over spatial ranges in the case of the  $x_i$  integrals. This is similar to the radiative transfer models of Mudgett and Richards [4,5], which were attempts to generalize the Kubelka-Munk [6] model to three dimensions. In matrix form the integral equation (4) becomes:

$$\begin{aligned}
 \mathbf{R}_{1Down} [I - t T_{2Up} t R_{3Up} t T_{2Down} t R_{1Down} - t R_{2Up} t R_{1Down}] &= \\
 [T_{1Up} t T_{2Up} t R_{3Up} t T_{2Down} t R_{1Down} + T_{1Up} t R_{2Up} t R_{1Down}] &+ \\
 \mathbf{R}_{2Down} t R_{3Up} t T_{2Down} t R_{1Down} \cdot \cdot \cdot \quad (6)
 \end{aligned}$$

where  $I$  is the unit matrix. Similarly, Eq. (5) becomes

$$\begin{aligned}
 \mathbf{R}_{2Down} [I - t R_{3Up} t R_{2Down}] &= [T_{1Up} t T_{2Up} t R_{3Up} t R_{2Down}] + \\
 \mathbf{R}_{1Down} t T_{2Up} t R_{3Up} t R_{2Down} \cdot \cdot \cdot \quad (7)
 \end{aligned}$$

In a more concise form these can be written as:

$$\mathbf{R}_{1Down} [I - A] + \mathbf{R}_{2Down} B = C, \quad (8)$$

$$\mathbf{R}_{1Down} D + \mathbf{R}_{2Down} [I - E] = F, \quad (9)$$

where the matrices A-F are given by:

$$A = t T_{2Up} t R_{3Up} t T_{2Down} t R_{1Down} + t R_{2Up} t R_{1Down} \quad (10)$$

$$B = - t R_{3Up} t T_{2Down} t R_{1Down} \quad (11)$$

$$C = T_{1Up} t T_{2Up} t R_{3Up} t T_{2Down} t R_{1Down} + T_{1Up} t R_{2Up} t R_{1Down} \quad (12)$$

$$D = - t T_{2Up} t R_{3Up} t R_{2Down} \quad (13)$$

$$E = t R_{3Up} t R_{2Down} \quad (14)$$

$$F = [T_{1Up} t T_{2Up} t R_{3Up} t R_{2Down}]. \quad (15)$$

The matrices A, B, C, D, E, F,  $\mathbf{R}_{1Down}$ , and  $\mathbf{R}_{2Down}$  don't commute. Therefore, the reflectivity problem reduces to a non-commutative algebra problem. After some simple matrix algebra, the exact solution for the renormalized reflectivity operators  $\mathbf{R}_{1Down}$  and  $\mathbf{R}_{2Down}$  are found to be:

$$\mathbf{R}_{1Down} = \{F - CB^{-1}(I-E)\} \{D - [I-A]B^{-1}(I-E)\}^{-1}, \quad (16)$$

$$\mathbf{R}_{2Down} = CB^{-1} - \{F - CB^{-1}(I-E)\} \{D - [I-A]B^{-1}(I-E)\}^{-1}. \quad (17)$$

The unrenormalized matrix operators (in black Times font) and the renormalized matrix operators (**in boldface red Helvetica font**) combine to give the total reflectivity matrix,  $R$ , including multiple scattering to all orders between the image front surface, the paper, and the pigment particles:

$$\begin{aligned}
 R &= R_{1Up} + [\{ (T_{1Up} + \mathbf{R}_{1Down}) t T_{2Up} + \mathbf{R}_{2Down} \} t R_{3Up} t T_{2Down} \\
 &+ (T_{1Up} + \mathbf{R}_{1Down}) t R_{2Up}] t T_{1Down}, \quad (18)
 \end{aligned}$$

where the renormalized reflection matrices are given by Eqs.(16) and (17). In the limit of zero pigment particle scattering this can be shown to reduce to the Williams-Clapper result.

The reflectivity  $R$  can be related to the CIELab color coordinates and tristimulus values in the well known manner (Billmeyer and Saltzman [8].)

Williams and Clapper [1] don't specify the functional forms of the reflection and transmission coefficients that appear in their analysis. As such, they recognize that the reflectivity expression functions as a formalism into which different physical models for transmission and reflection can be inserted. The same is true of the present analysis. Expressions for front surface transmittance and reflectance and paper reflectance valid for the Williams-Clapper model remains valid here. The new required expression is that for pigment layer transmittance and reflectance. Several different formulations can be given, depending on whether pigment particles are modeled as smooth or rough dielectric spheres, or particles of other shapes. Expressions based on

Mie theory of light scattering from smooth dielectric spheres can be inferred from Paine, et. al. [7].

## References

1. F. C. Williams and F. R. Clapper, *J.Opt. Soc. Am.*, **43**, 595 (1953).
2. K. Takahashi, *J. Imag. Sci. Technol.* **36**, 511 (1992).
3. Laurie M. Brown (editor), *Renormalization from Lorentz to Landau (and Beyond)*, Springer Verlag, New York NY (1993).
4. P. S. Mudgett and L. W. Richards, *Appl. Optics*, **10**, 1485 (1971).
5. P. S. Mudgett and L. W. Richards, *J. Colloid and Interf. Sci.* **39**, 551 (1972).
6. P. Kubelka and F. Munk, *Z. Tech. Physik*, **12**, 593 (1931).
7. A. J. Paine, F. Pontes, W. Mychajlowskij, D. Lousenberg, *J. Imaging Sci. Technol.* **37**, 5-12, (1993).
8. F. W. Billmeyer and M. Saltzman, *Principles of Color Technology*, Second Edition, Wiley Interscience, New York NY, 1981.